New Insights into the Pharmacokinetics and Metabolism of (R,S)-Ifosfamide in Cancer Patients Using a Population Pharmacokinetic-Metabolism Model

Marika Pasternyk Di Marco,[1] Irving W. Wainer,[1,2] Camille L. Granvil,[3] Gerald Batist,[3] and Murray P. Ducharme[1,4,5]

Received February 18, 2000; accepted March 13, 2000

Purpose. To describe the pharmacokinetics of R- and S-Ifosfamide (IFF), and their respective 2 and 3 N-dechloroethylated (DCE) metabolites (R2-, R3-, S2, S3-DCE-IFF) in cancer patients.

Methods. (R,S)-IFF was administered (1.5 g/m^2) daily for 5 days in 13 cancer patients. Plasma and urine samples were collected and analyzed using an enantioselective GC-MS method. An average of 97 observations per patient were simultaneously fitted using a pharmacokinetic-metabolism (PK-MB) model. A population PK analysis was performed using an iterative 2-stage method (IT2S).

Results. Auto-induction of IFF metabolism was observed over the 5 day period. Increases were seen in IFF clearance (R: 4 vs 7 L/h; S: 5 vs 10 L/h), and in the formation of DCE (R: 7 vs 9%; S: 14 vs 19%) and active metabolites (4-OHM-IFF; R: 71 vs 77%; S: 67 vs 71%). A novel finding of this analysis was that the renal excretion of the DCE metabolites was also induced.

Conclusions. This population PK-MB model for (R,S)-IFF may be useful in the optimization of patient care, and gives new insight into the metabolism of (R,S)-IFF.

KEY WORDS: (R,S)-Ifosfamide; R2-, R3-, S2-, S3-DCE-IFF; iterative-two stage analysis; pharmacokinetics.

INTRODUCTION

Estimating the pharmacokinetics (PKs) of oncology drugs, particularly those undergoing extensive metabolism, is a challenging but necessary process. Since a patient's starting regimen is usually calculated using the average population plasma clearance and volumes of distribution of the therapeutic agent, it is important to know the drug's PKs with the greatest possible precision. Population PK studies are very useful in this regard, as they provide clinicians with robust information that can be used in conjunction with Bayesian adaptive control to start therapies.

Ifosfamide (IFF) is a nitrogen mustard derivative widely used alone or in combination with other agents for multiple forms of tumors. Ifosfamide by itself is not active. It is a pro-drug converted *in vivo* via two metabolic pathways. One pathway is initiated by 4-hydroxylation and produces the cytotoxic isophosphoramide mustard metabolites (i.e., 4-OHM-IFF), while the other produces the N-dechloroethylated (DCE) metabolites (i.e., 2-DCE, 3-DCE-IFF) resulting from side chain oxidation (1). These last metabolites have been shown to be formed by CYP enzymes (CYP3A and CYP2B6) (2).

IFF is a chiral molecule (R,S) existing as R-IFF and S-IFF and is administered clinically as the racemate. The objective of this study is to propose a population pharmacokinetic-metabolism (PK-MB) model that can explain all observed plasma and urine concentrations of IFF enantiomers and their DCE metabolites in cancer patients when given by daily infusions for five days. The resulting PK-MB model may be used (with Bayesian adaptive control) to estimate the proportion of an IFF dose that would be 4-hydroxylated or N-dechloroethylated.

MATERIALS AND METHODS

Clinical Procedure

A group of 13 cancer patients with varying malignancies (such as ovarian, lung, breast and gastric adenocarcinomas) were included in this study. The mean ±SD weight, height and age of the patients enrolled in the study were 61.5 ± 18.3 kg, 165.0 ± 8.5 cm and 51 ± 10 years, respectively. This study protocol was approved by the Ethical Committee of McGill University. Written informed consent was obtained from each patient before entering the study protocol. Medications concomitantly administered to patients were not known to be significant inhibitors or inducers of CYP-mediated drug metabolism (ondansetron, acetaminophen and dextromethorphan). Dexamethasone was also given concomitantly to 5 out of the 13 patients. There was no significant difference observed in our PK analyses between those patients that took dexamethasone versus those that did not during this study.

IFF was administered by a 30 minute infusion at a dose of 1.5 g/m^2 daily for 5 days. Plasma samples were collected on day 1 at times 0 (pre-dose), 0.25, 0.47 (end of first infusion), 1, 1.5, 2.5, 4.5, 6.5, 24.5 hrs; on day 2 at 72.5 hrs; on day 3 at 96.5 hrs and on day 5 at times 120 (pre-dose), 120.25, 120.47 (end of fifth infusion), 121, 121.5, 122.5, 124.5, 126.5, and 144.5 hrs. Urine samples were collected during the following time-intervals after the beginning of the first dose infusion: 0–6, 6–12, 12–18, 18–24, 24–48, 48–72, 72–96, 96–102, 102–108, 108–114, and 114–120 hours.

Analytical Procedure

A validated gas chromatography (GC) method was used to analyze the extracted urine and plasma samples as previously described (3). The analytical assay was linear from a concentration range of 0.48 to 268 nmol/ml for each IFF enantiomer and

[1] Faculte de Pharmacie, Universite de Montreal, Montreal, Canada.
[2] Georgetown University Medical Center, Washington, DC, USA.
[3] Department of Oncology, McGill University, Montreal, Canada.
[4] Phoenix International Life Sciences, 2350 Cohen, St. Laurent H4R 2N6, Canada.
[5] To whom correspondence should be addressed. (e-mail: ducharmu@pils.com)

ABBREVIATIONS: A_1, relative affinity of CYP3A enzymes for substrate; A_2, relative affinity of CYP2B6 enzymes for substrate; CL_{DCE}, formation clearance to the DCE metabolites; CL_{4OHM}, formation clearance to the 4-OH metabolites; CL_R, renal clearance; CL_T, clearance total; GC-MS, gas chromatography with mass spectrometry; GLS, generalized least squares; Ind_{renal}, renal induction; K_{3A}, metabolite formation rate constant; K_{2B6}, metabolite formation rate constant; 4OHM, 4-hydroxy metabolites; T, time; T_{lag}, time lag.

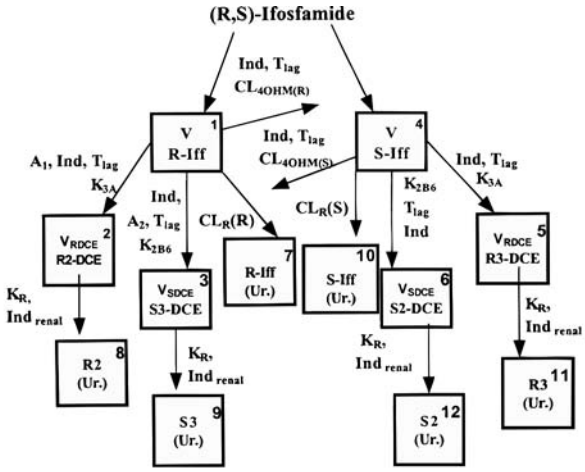

1 to 12: Compartment number (see differential equations)
A_1 and A_2= Relative affinity of enzymes for substrates
CL_{4OHM} = Formation clearance of IFF to 4-OH metabolites
$CL_R(R)$ = Renal clearance for R-IFF
$CL_R(S)$ = Renal clearance for S-IFF
K_{3A}, K_{2B6} = Metabolic formation rate constants
K_R = Renal elimation rate constant for the DCE metabolites

Ind = Metabolic induction process
Ind_{renal} = Renal induction process
Ur.: urine compartments
Tlag = Time before the induction process starts
V= Volume of distribution for R- and S-IFF
V_{SDCE}= Volume of distribution for the S2- and S3-DCE-IFF
V_{RDCE}= Volume of distribution for the R2- and R3-DCE-IFF

Fig. 1. Enantioselective pharmacokinetic-metabolism (PK-MB) (one compartment) model for (R, S)-Ifosfamide.

from 0.25 to 101 nmol/ml for each enantiomer of 2- and 3-DCE-IFF. The validation of the assay has been previously presented by Granvil *et al.* (3). Intra and inter-day coefficient of variation results (%CV) were less than 7%.

Pharmacokinetic Analysis

PK analyses were performed using compartmental techniques (4). The simplest model that best fitted simultaneously R-IFF, S-IFF, R2-, R3-, S2- and S3-DCE-IFF plasma concentrations and excreted urinary amounts was an enantioselective 1-compartment PK-MB model (Fig. 1). An average of 97 observations per patient were simultaneously fitted.

Granvil *et al.* (2) and Roy *et al.* (5) have shown that the enzymes responsible for the production of the R-DCE-IFF (R2- and R3-) and of the S-DCE-IFF (S2- and S3-) metabolites are CYP3A and CYP2B6, respectively. Because the formation rate constants associated with the formation of these DCE metabolites will be in any given patient correlated with their CYP3A and CYP2B6 activity, they are named K_{3A} and K_{2B6} in the PK-MB model.

Examples of other PK-MB models investigated for their quality of fit during the model discrimination process are presented in Fig. 2. None fitted the observed data properly based on visual inspection of graphs (concentrations versus time) and computations of pertinent statistical tests. The results of these analyses are presented in Table I. The model was improved with each proposed modification. This is presented by successive minimizations in the values of the AKAIKE information criterion test (AIC), minimum value of the objective function, average coefficient of determination and the residual errors.

Briefly, Model 1 consisted of fitting separate volumes of distribution (V) and renal elimination rate constants for all the different plasma observation types. Since preliminary estimates of V and of elimination rate constants for the DCE metabolites were similar, the model was simplified (Model 2). Auto-induction of metabolism was included in Model 3, while separate renal clearances for R- and S-IFF, and different volumes of distribution for R-DCE-IFF and S-DCE-IFF were added in Model 4.

Although the increase in the formation of the DCE metabolites were well described by Model 4, the plasma concentrations describing the elimination of these metabolites were consistently over-predicted. One possible explanation for this behavior was an induction of the renal secretion of the DCE metabolites over time. This process was therefore included in the final model (Fig. 1). Parameters fitted by this model were renal clearances for R- and S-IFF (CL_R in L/h), a single renal elimination rate constant for the DCE-IFF metabolites (K_R in h^{-1}), metabolic formation rate constants (K_{3A} and K_{2B6} in h^{-1}]), formation clearances to the 4-OH metabolites (CL_{4OHR} and $CL_{4OHS,}$ L/h), volumes of distribution for both R- and S-IFF (V in L) and for the DCE-IFF metabolites (V_{SDCE} [L] (R2-, R3-DCE, L) and V_{RDCE} [L] (S2-, S3-DCE-IFF)), and metabolic induction processes (Ind for the parameters K_{3A}, K_{2B6}, CL_{4OH} and K_R (Ind_{renal}) in %/hr). Clearances (CL) and volumes of distribution (V) were fitted for a body surface area (BSA) of 1.73 m^2. A lag time was also modeled (Tlag (h): duration of time before the start of the metabolic induction process once the first dose has been administered). CYP3A enzymes have been shown to preferentially metabolize S-IFF to R3-DCE-IFF versus R-IFF to R2-DCE-IFF (2). Differences in affinity between R -and S-IFF and CYP2B6 enzymes are also possible. Therefore, relative affinity factors (A_1, for K_{3A} and A_2 for K_{2B6}) were fitted.

The final PK-MB model may be described mathematically by the following series of differential equations, where dXi/dt refers to the change in the molar amounts of the drug in compartments i versus time:

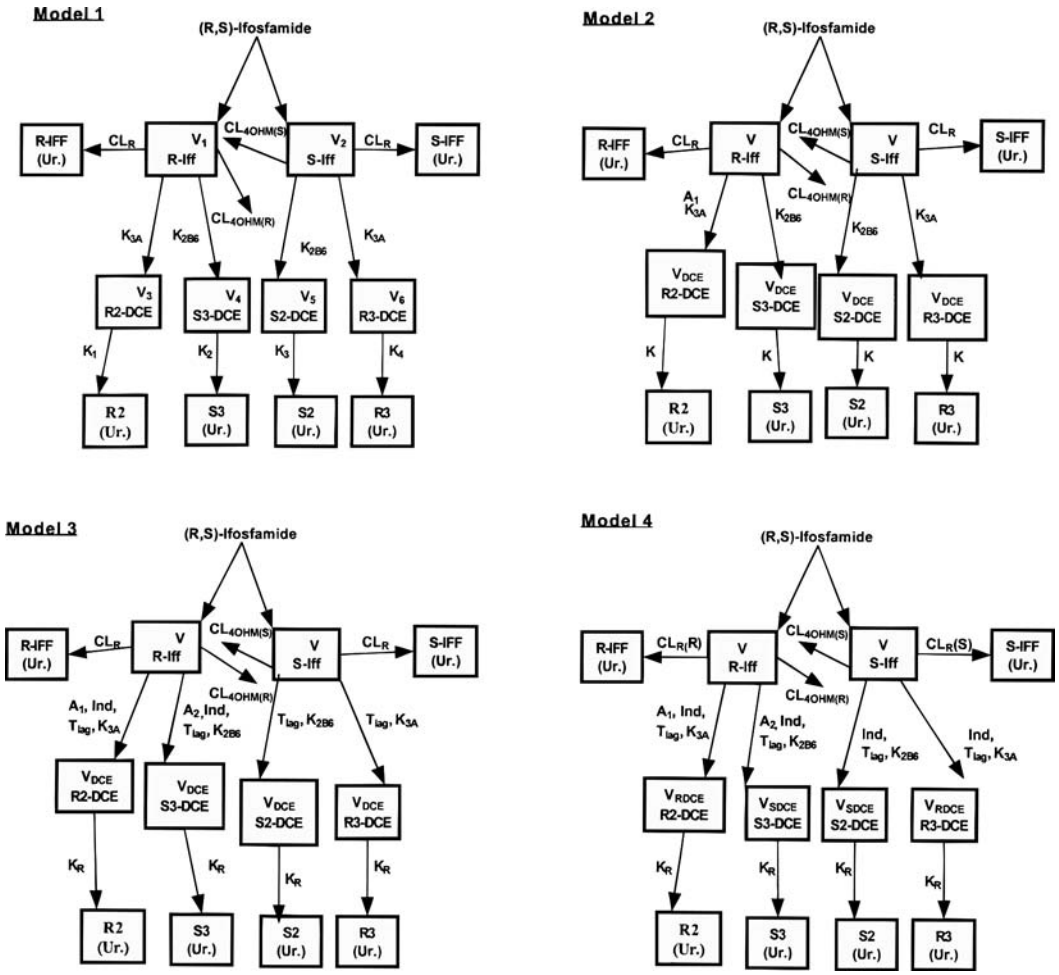

Fig. 2. Schematic representations of some of the rejected PK-MB models.

$$\frac{dX1}{dt} = \frac{R(1)}{2} - \left[\frac{CL_{R(R)}}{V} + (1 + Ind)\cdot(T - T_{lag})\cdot(K_{3A}\cdot A_1 + K_{2B6}\cdot A_2 + CL_{4OHM(R)})\right]\cdot X(1)$$

$$\frac{dX2}{dt} = A_1\cdot(1 + Ind)\cdot(T - Tlag)\cdot K_{3A}\cdot X(1) - (1 + Ind_{renal})\cdot(T - Tlag)\cdot K_R\cdot X(2)$$

$$\frac{dX3}{dt} = K_{2B6}\cdot A_2\cdot(1 + Ind)\cdot(T - T_{lag})\cdot X(1) - (1 + Ind_{renal})\cdot(T - Tlag)\cdot K_R\cdot X(3)$$

$$\frac{dX4}{dt} = \frac{R(1)}{2} - \left[\frac{CL_{R(S)}}{V} + (1 + Ind)\cdot(T - T_{lag})\right.$$

Table I. Parameters used in the Discrimination Process to Select the Final PK-MB Model (Models 1 to 4 Are Presented in Figure 2 and Model 5 in Figure 1)

			R^2 (median)		Residual error (CV%)			
Model #	AIC	OBJ	Plasma	urine	IFF (plasma)	DCE (plasma)	IFF (urine)	DCE (urine)
1	13906.14	801.22	0.823	0.782	17.0	25.0	47.0	75
2	13896.71	780.15	0.828	0.778	16.0	27.0	42.0	55
3	13758.18	687.76	0.919	0.8	11.2	13.5	41.0	60
4	13761.58	687.58	0.918	0.801	11.9	13.5	41.8	59.5
5	10512.1	572.36	0.919	0.838	11.8	6.8	31.4	44.2

AIC: AKAIKE information criterion test; OBJ: minimum value of the objective function; R^2: coefficient of determination values; CV: coefficient of variation.

$$\cdot (K_{3A} + K_{2B6} + CL_{4OHM(S)})\Big] \cdot X(4)$$

$$\frac{dX5}{dt} = (1 + Ind) \cdot (T - Tlag) \cdot K_{3A} \cdot X(4) - (1 + Ind_{renal}) \cdot (T - Tlag) \cdot K_R \cdot X(5)$$

$$\frac{dX6}{dt} = K_{2B6}\,(1 + Ind) \cdot (T - T_{lag}) \cdot X(4) - (1 + Ind_{renal}) \cdot (T - Tlag) \cdot K_R \cdot X(6)$$

$$\frac{dX7}{dt} = \frac{CL_{R(R)}}{V} \cdot X(1)$$

$$\frac{dX8}{dt} = (1 + Ind_{renal}) \cdot (T - Tlag) \cdot K_R \cdot X(2)$$

$$\frac{dX9}{dt} = (1 + Ind_{renal}) \cdot (T - Tlag) \cdot K_R \cdot X(3)$$

$$\frac{dX10}{dt} = \frac{CL_{R(S)}}{V} \cdot X(4)$$

$$\frac{dX11}{dt} = (1 + Ind_{renal}) \cdot (T - Tlag) \cdot K_R \cdot X(5)$$

$$\frac{dX12}{dt} = (1 + Ind_{renal}) \cdot (T - Tlag) \cdot K_R \cdot X(6)$$

where R(1) represents the intravenous dosing rate of (R,S)-IFF in molar units.

The following output equations were used to fit molar plasma concentrations and excreted urinary amounts of the R-IFF, S-IFF, and R2-, R3-, S2-, and S3-DCE-IFF metabolites simultaneously:

$$Y(1) = \frac{X(1)}{V} \qquad Y(7) = X(7) - Xstore(R(2),7)$$

$$Y(2) = \frac{X(2)}{V_{RDCE}} \qquad Y(8) = X(8) - Xstore(R(2),8)$$

$$Y(3) = \frac{X(3)}{V_{SDCE}} \qquad Y(9) = X(9) - Xstore(R(2),9)$$

$$Y(4) = \frac{X(4)}{V} \qquad Y(10) = X(10) - Xstore(R(2),10)$$

$$Y(5) = \frac{X(5)}{V_{RDCE}} \qquad Y(11) = X(11) - Xstore(R(2),11)$$

$$Y(6) = \frac{X(6)}{V_{SDCE}} \qquad Y(12) = X(12) - Xstore(R(2),12)$$

Individual PK estimates were derived using generalized least squares analysis (GLS, ADAPT-II) (6). The means of these estimates were used as beginning priors for the population pharmacokinetic analysis which was performed with an iterative 2-stage methodology (IT2S) (7). All plasma concentrations and urinary amounts of IFF and its DCE metabolites were weighted by the inverse of their variance ($W_j = 1/S_j^2$), which was calculated for each observation (Y_j) using the equation $S_j^2 = (b + a*Y_j)$ where a and b are the slope and intercept of each variance model, respectively. The slope (a) includes all errors associated with that particular observation type, and the intercept (b) is related to the limit of detection of the analytical assay for that particular observation type. These variance parameters were updated iteratively during the population analysis process.

Statistical analyses were performed with SYSTAT for Windows version 8 (SPSS Inc., 1998). Differences in the pharmacokinetic parameters between enantiomers (i.e., CL_R in the same patient for R-versus S-IFF) were estimated using a paired t-test. A value of $P < 0.05$ was determined *a priori* to be associated with statistical significance.

RESULTS

The proposed IFF model yielded a very good fit to the observed data and a one compartment PK model was found to be the simplest model to adequately describe the PKs of IFF. Graphic representations of fitted and observed molar plasma concentrations versus time for R-, S-, R2-DCE, R3-DCE, S2-DCE, and S3-DCE-IFF are presented in Figs. 3 and 4. These are examples of best (Fig. 3) and worst (Fig. 4) patient-fits. No obvious visual differences can be seen between these graphs, indicating an evenly distributed goodness of fit between patients.

Coefficient of determination values (R^2) associated with the modeling of plasma concentrations of R-IFF, S-IFF, R2-, R3-, S2-, and S3-DCE-IFF for all study patients were 0.996, 0.974, 0.938, 0.926, 0.992, 0.881, respectively. Examination of each graph of the weighted residuals versus the observed plasma concentrations for the parent drugs and the metabolites showed homoscedastic distributions with no systematic deviation or bias. The residual variability (includes all experimental errors and the intra-individual variability) in plasma concentrations for R- and S-IFF was 11.8%, while it was 6.8% for the DCE-IFF metabolites. These low numbers demonstrate that the population PK-MB model provided a good fit to the observed values, leaving the "unexplained" variability to a minimum.

Average (±SD) maximum observed plasma concentrations for the R-, and S-IFF enantiomers were taken directly from the observed data profiles and were found to be 123 ± 21 and 116 ± 19 μmol/L, respectively. The similarity between these numbers is consistent with both enantiomers having the same volume of distribution.

This study not only included plasma concentrations but individual cumulative urinary excretions as well. Graphs representing observed and fitted urinary excretions (from one representative patient) of R-IFF and S-IFF, as well as the four DCE metabolites are presented in Fig. 5. An excellent "goodness of fit" was observed for the urinary excretion data as demonstrated by R^2 values for R-IFF, S-IFF, R2-, R3-, S2-, and S3-DCE-IFF of 0.929, 1.0, 0.832, 1.0, 0.909, and 0.918, respectively. The residual variability in the urinary data for R- and S-IFF was 31.4% and 44.2% for the DCE-IFF metabolites. Urinary data typically have much more "noise" than plasma data and are usually associated with an "unexplained" variability ranging from 30 to 50% when the appropriate PK model is used.

Average population PK parameters are presented in Tables II and III, along with their associated inter-individual variability. One volume of distribution (V) was fitted for R- and S-IFF. In Model #1 (Fig. 2) two values were fitted but since their estimates were similar, the PK model was simplified to having the same V for both enantiomers.

Two distinct parameters were fitted for the volumes of distribution of the DCE metabolites based on the model buildup

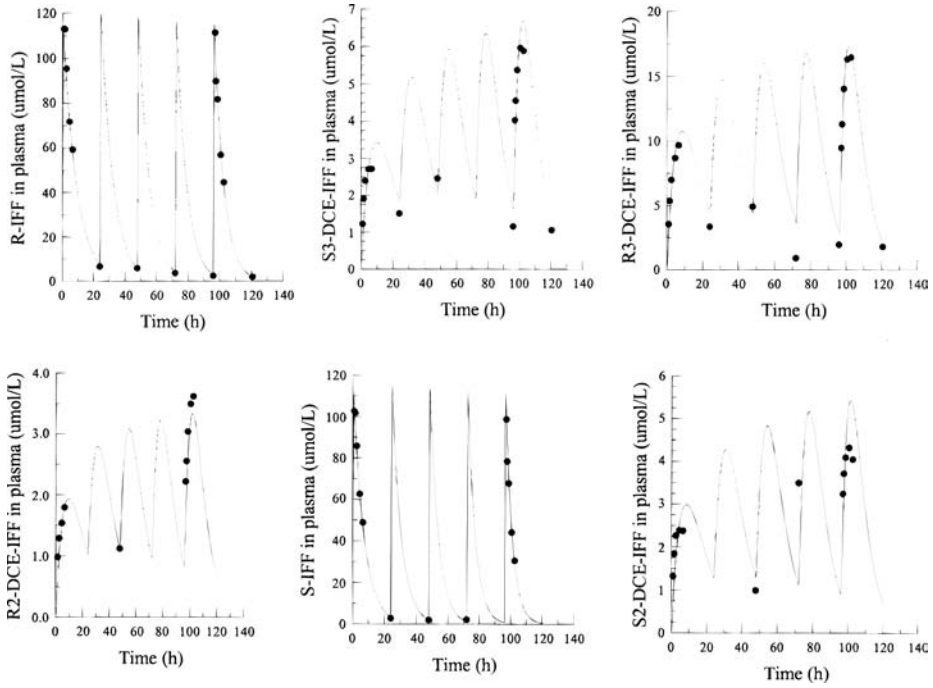

Fig. 3. Observed (•) and simultaneously fitted (−) plasma concentrations of R-IFF, S-IFF and R2-, R3-, S2-, S3-DCE-IFF in a representative patient.

process, V_{RDCE} and V_{SDCE}. Although the DCE metabolites appeared to distribute in the same volume of distribution (20.3 L and 19.2 L), the model could not be simplified to one volume as on an individual patient basis, the two volumes were different.

Metabolic formation rate constants were found to be almost 50% faster for K_{3A} (an index of CYP3A activity for IFF) than for K_{2B6} (an index of CYP2B6 activity for IFF), 0.011 to 0.006 hrs^{-1}. Renal clearance (CL_R) of the parent drug appeared to be slightly faster for S- versus R-IFF with values of 0.97 vs. 0.89 L/h, respectively. One distinct rate constant was fitted for the renal elimination of all the DCE metabolites, since individual values appeared to be the same during the model buildup process.

IFF is known to induce its own metabolism (auto-induction) (8). This process was included in the PK-MB model, as a percent increase in clearance for every hour (induction factor, Ind) past a certain duration of time (Tlag). This last parameter had to be present in the PK-MB model because up-regulation

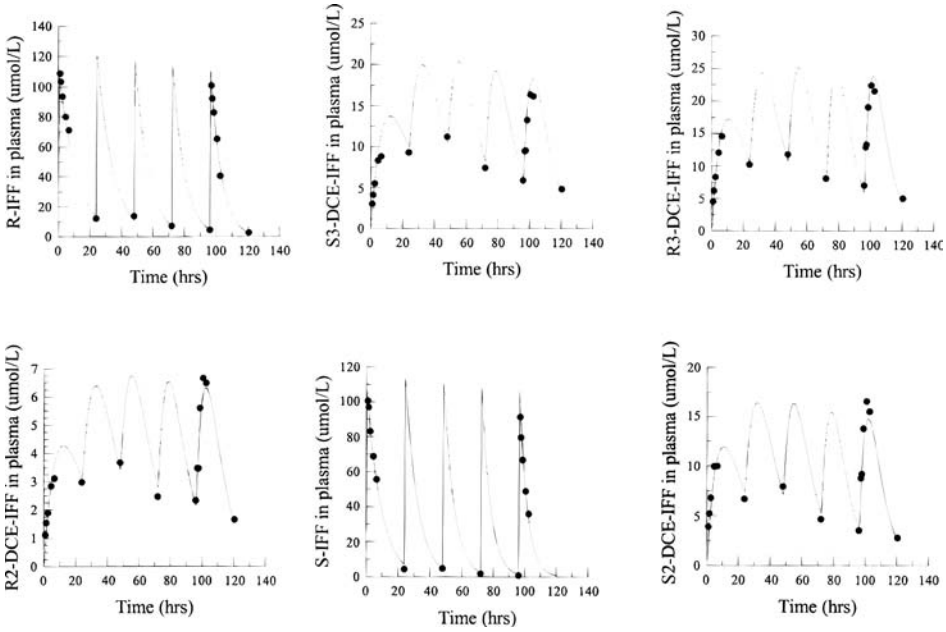

Fig. 4. Observed (•) and simultaneously fitted (−) plasma concentrations of R-IFF, S-IFF and R2-, R3-, S2-, S3-DCE-IFF in a representative patient.

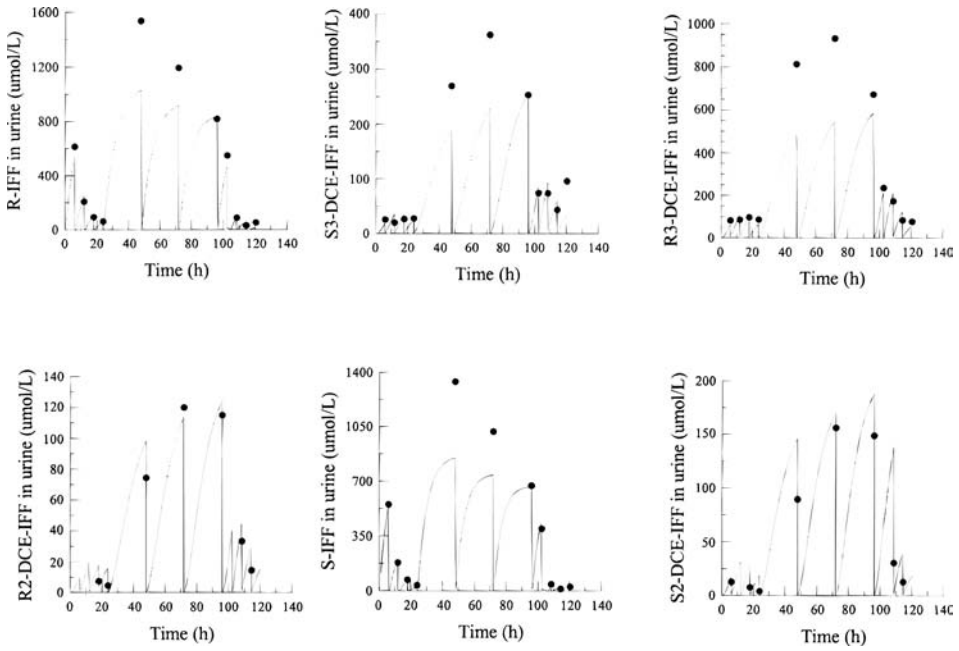

Fig. 5. Observed (•) and simultaneously fitted (−) urine amounts of R-IFF, S-IFF and R2-, R3-, S2-, S3-DCE-IFF in a representative patient.

of enzyme production does not immediately begin at the initiation of IFF treatment. A similar type of lag has been observed for other enzyme inducers such as cyclophosphamide which is metabolized in part by CYP2B6/CYP3A (9), and carbamazepine (10) which is metabolized by CYP3A. With IFF, autoinduction of clearance started on average 10 hours after the first dose and proceeded at an increase of 1.5, 2.15 and 0.9 % per hour for K_{3A}, K_{2B6} and Ind_{renal}, respectively.

Relative affinities of enzymes to substrates were also fitted in the PK-MB model to determine which of the enzymes showed more affinity for the respective enantiomers of IFF. Being a "relative" value, the affinity associated with the S-IFF was the one *a priori* considered to be at 100%. Results show (Table II) that K_{3A} and K_{2B6} had less relative affinity for R-IFF (22.6% and 69.4%, respectively) compared with S-IFF. These results are in agreement with previously published *in vitro* findings (2).

Population fitted PK parameters presented in Tables II and III were used to calculate the percentage of the administered dose of R- and S-IFF eliminated through different metabolic or elimination pathways (Tables IV and V).

Table II. Average Population Fitted Pharmacokinetic Parameters and Their Associated Inter-individual Variability Values (CV%)

Fitted PK parameters		Mean	CV%	P value
V (L)*	R-IFF S-IFF	46.2	7.7	
V_{RDCE} (L)*	R2-DCE-IFF R3-DCE-IFF	20.27	29.1	
V_{SDCE} (L)*	S2-DCE-IFF S3-DCE-IFF	19.24	28.9	<0.05
K_{3A} (h^{-1})		0.011	49.3	<0.05
K_{2B6} (h^{-1})		0.006	44.4	
CL_{4OHM} (L/h)*	R-IFF	2.95	21.2	<0.05
	S-IFF	3.6	23.7	
CL_R (L/h)*	R-IFF	0.89	29.6	<0.05
	S-IFF	0.97	28.5	

* Parameters fitted for a body surface area (BSA) of 1.73 m^2 V: Volumes of distribution; K_{3A}: metabolite formation rate constant; K_{2B6}: metabolite formation rate constant; CL_{4OHM}: formation clearance to the 4-OH metabolites; CL_R: renal clearance of R- and S-IFF.

Table III. Average Population Fitted Pharmacokinetic Parameters and Their Associated Inter-individual Variability Values (CV%)

Fitted PK parameters		Mean	CV%
Kr (h^{-1})	R2-DCE-IFF R3-DCE-IFF S2-DCE-IFF S3-DCE-IFF	0.07	31.5
Ind (% per hour)	K_{3A}	1.5	19.8
	K_{2B6}	2.15	42.0
	Ind_{renal}	0.9	44.1
	CL_{4OHM}	1.1	28.0
T_{lag} (h)	K_{3A}, K_{2B6}, CL_{4OHM}, Ind_{renal}	10.5	57.7
A_1 (K_{3A}, %)	R-IFF	22.6	19.8
	S-IFF	100 (reference)	
A_2 (K_{2B6}, %)	R-IFF	69.4	42.1
	S-IFF	100 (reference)	

Kr: Renal elimination rate constant of the DCE metabolites; Ind: metabolic induction; T_{lag}: time before induction starts; A_1 (K_{3A}) and A_2 (K_{2B6}): relative affinity of enzymes for substrates.

Table IV. Clearances of R- and S-IFF After 1 and 5 Daily Administrations of (R,S)-IFF

Total clearance (L/h)	DAY 1	DAY 5
R-IFF	4.1 ± 0.65	7.2 ± 1.5
S-IFF	5.3 ± 0.99	9.6 ± 2.17

Note: Mean ± SD.

Table V. Comparison of the Percent Formation of Metabolites from R-and S-IFF After 1 and 5 Daily Administrations of (R,S)-IFF

Percent formation of metabolites from a dose of (R,S)-IFF	DAY 1	DAY 5
R-DCE-IFF	6.9 ± 2.73	9.1 ± 3.74
S-DCE-IFF	14.1 ± 5.32	18.7 ± 4.47
R-4OH-IFF	71.1 ± 6.40	77 ± 7.08
S-4OH-IFF	67.2 ± 6.92	70.6 ± 7.20

Note: Mean ± SD.

DISCUSSION

IFF is a pro-drug that is administered clinically as a racemic (50:50) mixture of R- and S-IFF (11,12). Each mole of IFF metabolized by the dechloroethylated pathway produces one mole of the DCE metabolites and one mole of chloroacetaldelhyde (13).

In an *in vitro* model using cDNA enzymes, CYP3A were found to be the most potent enzymes to transform R- and S-IFF to the R2- and R3-DCE-IFF metabolites, while CYP2B6 were found to be mostly responsible for the formation of S2- and S3-DCE metabolites (2). In our *in vivo* PK-MB model (Fig. 1), the activities of CYP3A and CYP2B6 enzymes are represented by formation rate constants to the DCE metabolites from the available concentrations of parent R- and S-IFF. For reading and simplicity purposes, these formation rate constants are named K_{3A} and K_{2B6} and proposed to be indexes of CYP3A and CYP2B6 activities in any given patient for IFF.

These formation rate constants could not have been robustly discriminated from the elimination rate constants of the metabolites without the simultaneous modeling of the urine data. In this study, we found that on the first day of therapy, the elimination rate constant for the DCE metabolites was actually larger than their formation rate constant. Therefore, the terminal "elimination" slope of the plasma concentrations versus time curves of the metabolites is a reflection of their formation and not their elimination. This observation is an example of a "flip-flop" phenomenon since the terminal slope is always representative of the rate limiting step, in this case the formation of the metabolites (14).

Because of the auto-induction process in which CYP3A and CYP2B6 are up-regulated, the picture is somewhat complicated after 5 days of therapy. The "flip-flop" observed at day one no longer occurs because formation of the metabolites is now faster than their elimination. This complicated picture highlights two key issues in the characterization of IFF PKs: the simultaneous fitting of all observed concentrations and the availability of urine and plasma observations. In addition to metabolic clearance to the DCE-IFF metabolites, R- and S-IFF are passively eliminated (15). Since clearances are additive, the data from this study demonstrates that the proportion of R- and S-IFF eliminated unchanged in the urine was 21.9 and 18.7%, respectively.

IFF is not only metabolized to DCE-IFF metabolites (R2-, R3- and S2-, S3-DCE-IFF) but is also transformed through the initial CYP mediated formation of 4-OH-IFF into cytotoxic and inactive metabolites (16). We have considered these metabolites produced from 4-hydroxylation as one group of compounds, and have labeled them 4-OHM-IFF. These metabolites are very difficult to detect reliably in the plasma. While some researchers have been able to measure their plasma concentrations, these metabolites may be taken up by cells and degraded to other metabolites too quickly to be sure that their formation percentage is reliably determined by fitting plasma concentrations only (16).

IFF is eliminated and/or degraded in the organism via three different pathways. It is excreted 1) unchanged as the parent compound in the urine, 2) transformed into DCE metabolites and then excreted in the urine, or 3) transformed by 4-hydroxylation into active (i.e., 4-OHM-IFF) metabolites and then excreted in the urine. Since clearances are additive, the formation clearance of IFF to the 4-OHM-IFF can easily be computed by the model for each patient by subtracting all accounted for elimination/degradation pathways from the total clearance, e.g., $CL_T = CL_{DCE} + CL_{4OHM} + CL_R$. Since doses and clearances are directly related, the percent formation through a specific pathway is the ratio of the clearance through this pathway with the total clearance (i.e., $\%4\text{-OHM(R)} = CL_{4OHM}(R)/CL_T(R)$). Thus, the proposed PK-MB model can estimate the proportion of an administered dose of IFF which will be converted to "active" (4-OHM) and "toxic" (DCE) metabolic pathways.

Two additional factors that complicate the pharmacokinetics of IFF have been built into the proposed PK-MB model. First, as has been observed with cyclophosphamide and carbamazepine (17–18), IFF induces its own metabolism. The induction of IFF metabolism is demonstrated by the fact that the observed data points between the Cmax and trough values decrease faster on day 5 than on the first day of administration, Figs. 3 and 4. The observed increase in IFF clearance is most probably the result of an up-regulation in enzymatic activity (i.e., CYP3A and CYP2B6) which is indicated by a corresponding increase in the formation of the DCE metabolites between day 1 and 5. For example, peak concentrations of R2-DCE-IFF are significantly lower on day 1 than on day 5 (Fig. 4). This could not be explained by the multiple daily administrations, as PK models not incorporating this auto-induction (Table I, Model 1 and 2) could not fit consistently the observed concentrations.

The renal elimination of DCE metabolites is the other complicating process that became apparent during the construction of the PK-MB model. In Figs. 3 and 4, there is a decrease in the trough values (concentrations in the plasma before the next administration of IFF) for all the DCE metabolites. Assuming that the renal elimination of the DCE metabolites is a passive process and is constant, there is an increase in the formation of the DCE metabolites without seeing a concomitant increase in the whole concentration versus time curves. This phenomenon is

consistent with the DCE metabolites being renally eliminated not just by a passive mechanism (i.e., filtration) but by an active one as well (i.e., secretion). Observed plasma concentrations and excreted urinary amounts of the DCE metabolites could only be described appropriately if their renal elimination was increasing over time. Therefore, we hypothesized from these results that the DCE metabolites were eliminated by an auto-inducible renal secretion process. This process could be associated with the activity of drug transporter proteins (such as the P-glycoprotein subfamily of transporters) which are involved in the renal secretion of drugs (i.e., digoxin and many anticancer agents) (19–20).

We have described in this paper an extensive PK study of IFF and its DCE metabolites over 5 consecutive days of administrations. Our results are consistent with that of others who have only looked at partial aspects of IFF PK studies. For instance, Kaijser *et al.* (21) have reported a V of 42.8 L and our paper presents a V of 46.2 L, while Allen *et al.* (22) reported a renal clearance of 0.98 L/h while our calculated value was 0.97 L/h (mean of R and S-IFF).

The clinically important ramifications of this research are that the proposed model can be used with Bayesian adaptive control by clinicians at the initiation of therapy to predict the proportion of a dose that will be transformed via the "active" and "toxic" metabolic pathways. This would allow dose adjustments and optimization of therapeutic regimens. For example, this model could have been used to predict that pretreatment of a patient with phenytoin would have resulted in an increased formation of the "toxic" metabolites (23).

In conclusion, the proposed PK-MB model not only describes the PKs of IFF, but also provides an index of a patient's CYP activities. Inclusion of these processes decreases the "unexplained" variability which was found to be low in this study (11.8 and 6.8% for R-, S-IFF and for R2-, R3-, S2, S3-DCE-IFF, respectively). The proposed PK-MB model can predict from the plasma concentrations of the first IFF administration what the total exposure of the patient to the 4-hydroxylated and N-dechloroethylated metabolites will be over the five days of future administrations.

ACKNOWLEDGMENTS

This study has been possible in part by a generous contribution of BioChem Pharma Inc., supporting M. Pasternyk Di Marco's PhD studies.

REFERENCES

1. C. P. Granvil, J. Ducharme, B.-Leyland Jones, M. Trudeau, and I. W. Wainer. Stereoselective pharmacokinetics of ifosfamide and its 2- and 3-*N*-dechloroethylated metabolites in female cancer patients. *Cancer Chemother. Pharmacol.* **37**:451–456 (1996).
2. C. P. Granvil, A. Madan, M. Sharkawi, A. Parkinson, and I. W. Wainer. Role of CYP2B6 and CYP3A4 in the *in vitro* N-Dechloroethylation of R- and S-Ifosfamide in human liver. *Drug Metab. Dispos.* **27**:533–541 (1999).
3. C. P. Granvil, B. Gehrcke, W. A. Konig, and I. W. Wainer. Determination of the enantiomers of ifosfamide and its 2- and 3-N-dechloroethylated metabolites in plasma and urine using enantioselective gas chromatography with mass spectrometric detection. *J. Chromatogr.* **622**:21–31 (1993).
4. M. Gibaldi and D. Perrier. *Pharmacokinetics*, 2nd ed. Marcel Dekker Inc., New York, 1982.
5. P. Roy, O. Tretyakov, J. Wright, and D. J. Waxman. Stereoselective metabolism of ifosfamide by human P-450s 3A4 and 2B6. Favorable metabolic properties of R-enantiomer. *Drug Metab. Dispos.* Nov; **27**:1309–1318 (1999).
6. D. Z. D'Argenio and A. Schumitzky. *ADAPT-II user's guide*. Biomedical Simulations Resource. University of Southern California, Los Angeles, CA: 1995.
7. D. Collins and A. Forrest. *IT2S user's guide*. State University of New York at Buffalo, Buffalo, NY: 1995.
8. V. Boddy, M. Cole, A. D. J. Pearson, and J. R. Idle. The kinetics of the auto-induction of ifosfamide metabolism during continuous infusion. *Cancer Chemother. Pharmacol.* **36**:53–60 (1995).
9. L. Gervot, B. Rochat, J. C. Gautier, F. Bohnenstengel, H. Kroemer, V. de Berardinis, H. Martin, P. Beaune, and I. de Waziers. Human CYP2B6: expression, inducibility and catalytic activities. *Pharmacogenetics.* **9**:295–306 (1999).
10. M. Eichelbaum, T. Tomson, G. Tybring, and L. Bertilsson. Carbamazepine metabolism in man. Induction and pharmacogenetic aspects. *Clin. Pharmacokinet.* **10:**80–90 (1985).
11. I. W. Wainer, J. Ducharme, C. P. Granvil, M. Trudeau, and B. Leyland Jones. Ifosfamide stereoselective dechloroethylation and neurotoxicity. *Lancet.* **343**:982–983 (1994).
12. P. B. Farmer. Enantiomers of cyclophosphamide and iphosphamide. *Biochem. Pharmacol.* **37**:145–148 (1988).
13. E. G. C. Brain, L. J. Yu, K. Gustafsson, P. Drewes, and D. J. Waxman. Modulation of P450-dependent ifosfamide pharmacokinetics: a better understanding of drug activation in vivo. *Br. J. Cancer.* **77**:1768–1776 (1998).
14. L. Shargel and A. Yu. *Applied Biopharmaceutics and Pharmacokinetics*; 4th ed. Appleton and Lange, Stanford, Connecticut, 1999, pp. 231–232.
15. I. W. Wainer, J. Ducharme, and C. P. Granvil. The N-dechloroethylation of ifosfamide: using stereochemistry to obtain an accurate picture of a clinically relevant metabolic pathway. *Cancer Chemother. Pharmaco.* **37**:332–6 (1996).
16. R. F. Struck, D. M. McCain, S. W. Tendian, and K. H. Tillery. Quantification of 4-hydroxyifosfamide in plasma of ifosfamide treated mice. *Cancer Chemother. Pharmacol.* **40**:57–59 (1997).
17. M. D'Incalci G. Bolis, T. Facchinetti, C. Mangioni, L. Morasca, P. Morazzoni, and M. Salmona. Decreased half-life of cyclophosphamide in patients under continual treatment. *Eur. J. Cancer.* **13**:7–10 (1979).
18. T. B. Kudriakova, L. A. Sirota, G. I. Rozova, and V. A. Gorkov. Autoinduction and steady-state pharmacokinetics of carbamazepine and its major metabolites. *Br. J. Clin. Pharmacol.* **33**:611–615 (1992).
19. O. Fardel, V. Lecureur, and A. Guillouzo, The P-glycoprotein multidrug transporter. *Gen. Pharmacol.* **27**:1283–1291 (1996).
20. D. M. Bradshaw and R. J. Arceci. Clinical relevance of transmembrane drug efflux as a mechanism of multidrug resistance. *J.Clin Oncol.* **16**:3674–3690 (1998).
21. G. P. Kaijser, J. H. Beijnen, A. Bult, and W. J. M. Underberg. Ifosfamide Metabolism and Pharmacokinetics. *Anticancer Res.* **14**:517–532 (1994).
22. L. M. Allen, P.J. Creaven. Pharmacokinetics of Ifosfamide. *Clin. Pharmacol. Ther.* **17**:492–498 (1975).
23. M. P. Ducharme, M. L. Bernstein, C. P. Granvil, B. Gehrcke, and I. W. Wainer. Phenytoin-induced alteration in the N-dechloroethylation of ifosfamide stereoisomers. *Cancer Chemother Pharmacol.* **40**:531–533 (1997).